

M(II)(H₂O)₂ (5,5'-dimethyl-2,2'-bipyridine)(fumarato) [M = Co and Zn] complexes bearing a unique distorted trigonal-prismatic geometry and displaying 2D supramolecular structures



Antonio Téllez-López^a, Jonathan Jaramillo-García^a, Rogelio Martínez-Domínguez^a, Raúl A. Morales-Luckie^b, Miguel A. Camacho-Lopez^c, Roberto Escudero^d, Víctor Sánchez-Mendieta^{a,*}

^a Facultad de Química, Universidad Autónoma del Estado de México, Paseo Colón y Paseo Tollocan, Toluca, Estado de México 50120, Mexico

^b Centro Conjunto de Investigación en Química Sustentable UAEM-UNAM, Carretera Toluca-Ixtlahuaca Km. 14.5, Tlachaloya, Toluca, Estado de México, Mexico

^c Laboratorio de Fotomedicina, Biofotónica y Espectroscopia Láser de Pulsos Ultracortos, Facultad de Medicina, Universidad Autónoma del Estado de México, Paseo Tollocan s/n esq. Jesús Carranza, Toluca, Estado de México 50120, Mexico

^d Instituto de Investigaciones en Materiales, Universidad Nacional Autónoma de México, Apartado Postal 70-360, México, Distrito Federal 04510, Mexico

ARTICLE INFO

Article history:

Received 21 May 2015

Accepted 24 August 2015

Available online 31 August 2015

Keywords:

Cobalt complexes

Zinc complexes

Trigonal-prismatic geometry

Supramolecular network

Fumarato

ABSTRACT

Novel M(II)(H₂O)₂(dbpy)(fum) complexes, M = Co (**1**) and M = Zn (**2**); where: dbpy = 5,5'-dimethyl-2,2'-bipyridine, fum = fumarato; were obtained by simple one-pot solution reactions at ambient conditions, and structurally characterized by elemental analysis, IR spectroscopy and X-ray single crystal diffraction. In both complexes, the Co(II) and Zn(II) ions exhibit an uncommon six-coordinated distorted trigonal-prismatic geometry, especially for complexes having mono-dentate and bi-dentate innocent ligands. These are the first examples of metaprism complexes with aqua ligands in their coordination spheres. Moreover, the η¹:η¹ non-bridging coordination mode of fumarato ligand appears for the first time in these type of mononuclear complexes. In addition, the solid-state self-assembly of the mononuclear structures of **1** and **2**, mainly throughout hydrogen bonding, give rise to 2D supramolecular wrinkle-sheet type frameworks. These extended structures seem to be the driving force for the unusual coordination geometry obtained in both complexes. Magnetic properties measurements reveal that complex **1** exhibits weak antiferromagnetic ordering with θ_(C-W) = -14 K and an E₁ = 0.24 cm⁻¹ according to Curie-Weiss model and Rueff phenomenological approach, respectively; whereas, complex **2** displays blue fluorescence in the solid-state.

© 2015 Elsevier Ltd. All rights reserved.

1. Introduction

As it is well known, transition metal six-coordination continues to be ruled by octahedral geometries. Nonetheless, approximately in the last two decades, there have been a series of transition-metal complexes in which the trigonal-prismatic geometry appears, mainly due to the use of non-innocent multi-chelating ligands and by forcing this geometry by ligand design [1–3] but also, in fewer cases, this geometry has been exhibited in complexes using innocent bidentate ligands, such as bipyridine and acac, an even in complexes with monodentate ligands [4–6]. In addition, several complexes have been obtained with geometries intermediate between the octahedron and the trigonal prism, named as metaprisms [7]. These kinds of compounds are usually described by their

degree of distortion interconversion path between the two ideal polyhedra, which is known as the Bailar twist [7]. The trigonal-prismatic coordination geometry has gained interest due to the presence of this type of geometry in Mo and W active sites in enzymes [8], and also, appears as a transition state in the intramolecular racemization reactions of octahedral tris(chelate) complexes [9].

It has been shown that the number, or relative abundance, of trigonal-prismatic complexes for the transition metals is scarcely 1.0% of the six-coordinated metal centers [7]. Also, it has been found that the distribution of this type of geometry among the transition metals is highly inhomogeneous; the frequency of trigonal-prismatic structures is highest for transition metals in groups 3 and 4, Ag and group 12. In addition, there are some metals in groups 5, 6 and 7, and Fe, that also contribute with some examples of trigonal-prismatic complexes. Thus, most of the complexes exhibiting trigonal prism geometry belong to those metal–ligand combinations having soft donor atoms and central metal in a high

* Corresponding author.

E-mail address: vsanchezm@uamex.mx (V. Sánchez-Mendieta).

oxidation state, with d^0 , d^1 and d^2 configurations. Therefore, mixed ligands trigonal-prismatic complexes of Co, and, to some extent of Zn, using innocent bidentate ligands are still considered rare. Even more, to our knowledge there are not examples reported in literature about metaprisms complexes with aqua ligands in their structures.

While searching for novel coordination polymers based on fumarate and dialkyl-bipyridine ligands, the X-ray diffraction structures of complexes **1** and **2** were determined and studied. Several strategies have been developed to synthesize bivalent-transition metal mixed ligands complexes containing nitrogen and oxygen donor ligands [10]. Among the most used bridging ligands for transition metal ions are the dicarboxylate ligands [11]. In particular, fumarate ligand has been extensively used for the formation of complexes [12] and coordination polymers [13]. We selected this ion-bridging ligand due to its simple chemical structure and its dual chemical functionality, which allow generating complexes or polymers, depending on its coordination modes. The use of 2,2'-bipyridine as ancillary ligand had become relevant in our previous studies on coordination polymers [14]; therefore, we decided to keep using one of the most studied nitrogen donor ligand [15], and just varying the alkyl-substituent on it, in order to verify the possible influence of the steric hindrance on the complexes crystalline structures.

The field of supramolecular chemistry focuses on the non-covalent interactions between molecules that give rise to molecular recognition and self-assembly processes [16]. Self-assembly of small molecules, compounds or complexes, has demonstrated to be an appreciated process for synthesizing large structures with a minimum effort. Moreover, crystal engineering refers to the construction of crystal structures from organic and metal-organic compounds using design principles that come from an understanding of the intermolecular interactions in the molecular solids [17]. Supramolecular frameworks based on metal ions and organic ligands have gained interest recently due to their fascinating structural diversity and their potential applications in catalysis, sensors, porosity and non-linear optics [18,19].

Herein, we describe the synthesis, crystal structures details and properties of complexes **1** and **2**, exhibiting unusual distorted trigonal-prismatic coordination geometries that include aqua ligands and a unique $\eta^1:\eta^1$ non-bridging coordination mode of fumarate, as well as 2D supramolecular arrays through hydrogen bonding.

2. Experimental

2.1. Materials and methods

All chemicals were of analytical grade, purchased commercially (Aldrich) and were used without further purification. All syntheses were carried out in aerobic and ambient conditions.

2.2. Preparation of complexes

2.2.1. Synthesis of $\text{Co}(\text{H}_2\text{O})_2(\text{dbpy})(\text{fum})$ (**1**)

A methanol solution (10 ml) of 5,5'-dimethyl-2,2'-bipyridine (0.0921 g; 0.5 mmol) was added to an aqueous solution (5 ml) of sodium fumarate (0.0800 g; 0.5 mmol), while stirring. To this solution, $\text{Co}(\text{NO}_3)_2 \cdot 6\text{H}_2\text{O}$ (0.1455 g; 0.5 mmol) in 5 ml of de-ionized water was added. Initially, a yellow color solution was obtained, which turned to dark-orange with time. After three days, large dark-magenta crystals were obtained then filtered, washed with a 50:50 deionized water-methanol solution and air-dried. Yield: 68% based on metal precursor. *Anal. Calc.* for $\text{C}_{16}\text{H}_{18}\text{CoN}_2\text{O}_6$ (FW = 393.25): C, 48.84; H, 4.61; N, 7.12. Found: C, 48.75; H,

4.63; N, 7.12%. IR (cm^{-1}): 3249 (s, br), 2920 (m), 1713 (w), 1540 (s), 1482 (m), 1424 (m), 1374 (s), 1252 (m), 1208 (m), 1055 (m), 1011 (m), 824 (m), 732 (m), 678 (s, sh), 555 (m, sh), 418 (m).

2.2.2. Synthesis of $\text{Zn}(\text{H}_2\text{O})_2(\text{dbpy})(\text{fum})$ (**2**)

A methanol solution (10 ml) of 5,5'-dimethyl-2,2'-bipyridine (0.0184 g; 0.1 mmol) was added to an aqueous solution (5 ml) of sodium fumarate (0.0160 g; 0.1 mmol), while stirring. To this solution, $\text{Zn}(\text{NO}_3)_2 \cdot 6\text{H}_2\text{O}$ (0.0297 g; 0.1 mmol) in 5 ml of de-ionized water was added. A transparent solution was obtained. After two days, large colorless crystals were obtained, then filtered, washed with a 50:50 deionized water-methanol solution and air-dried. Yield: 56% based on metal precursor. *Anal. Calc.* for $\text{C}_{16}\text{H}_{18}\text{ZnN}_2\text{O}_6$ (FW = 399.69): C, 48.24; H, 4.52; N, 7.03. Found: C, 48.61; H, 4.28; N, 7.21%. IR (cm^{-1}): 3244 (vs br), 2969 (s, br), 2920 (s, br), 1694 (m), 1615 (w), 1556 (s), 1483 (m), 1380 (s), 1247 (m), 1208 (m), 1163 (m, sh), 1051 (m), 1006 (m, sh), 830 (vm), 732 (m), 678 (m), 560 (vm), 472 (m), 418 (m).

2.3. Physical measurements

Elemental analyses for C, H, N were carried out for standard methods using a Vario Micro-Cube analyzer. IR spectra of the complexes were determined as KBr disks in an Avatar 360 FT-IR E.S.P. Nicolet spectrophotometer from 4000–400 cm^{-1} . Thermogravimetric analyses were performed in a TA Instruments equipment, under N_2 atmosphere, at a heating rate of 10 $^\circ\text{C min}^{-1}$, from 20 to 800 $^\circ\text{C}$. Magnetic characteristics of the complex **1** were determined in a MPMS Quantum Design magnetometer with measurements performed at zero field cooling (ZFC) and field cooling (FC) from 2 to 300 K and decreasing. The applied magnetic field was 100 Oe, and the total diamagnetic corrections were estimated using Pascal's constants as $-250 \times 10^{-6} \text{ cm}^3 \text{ mol}^{-1}$. PL emission spectra of complex **2** were measured in solid samples at room temperature using a Horiba Jovin Yvon Spectrofluorimeter (Fluoromax-P) with dual excitation and emission monochromators.

2.4. X-ray crystallography

Crystallographic data for **1** and **2** were collected on a Bruker SMART APEX DUO three-circle diffractometer equipped with an Apex II CCD detector using Mo $K\alpha$ ($\lambda = 0.71073 \text{ \AA}$, Incoatec μS microsource) at 100 K [20]. The crystals were coated with hydrocarbon oil, picked up with a nylon loop, and immediately mounted in the cold nitrogen stream (100 K) of the diffractometer. The structures were solved by direct methods (SHELXS-97) and refined by full-matrix least-squares on F^2 [21] using the shelXle GUI [22]. The hydrogen atoms of the C–H bonds were placed in idealized positions whereas the hydrogen atoms from H_2O moieties were localized from the difference electron density map, and their position was refined with U_{iso} tied to the parent atom with distance restraints. The disordered hydrogens were refined using distance restraints (DFIX). The crystallographic data and refinement details for the two complexes are summarized in Table 1.

3. Results and discussion

3.1. Synthesis

Using a very simple methodology of self-assembling solution reactions, equivalent amounts of sodium fumarate (fum), 5,5'-dimethyl-2,2'-bipyridine (dbpy) and $\text{Co}(\text{NO}_3)_2 \cdot 6\text{H}_2\text{O}$ and $\text{Zn}(\text{NO}_3)_2 \cdot 6\text{H}_2\text{O}$, respectively, were mixed in a water-methanol solution, under ambient conditions. Slow evaporation of solvents

Table 1
Crystal data and structure refinement parameters for **1** and **2**.

	1	2
Empirical formula	C ₁₆ H ₁₈ CoN ₂ O ₆	C ₁₆ H ₁₈ N ₂ O ₆ Zn
Formula weight	393.25	399.69
T (K)	100(2)	
Wavelength (Å)	0.71073	
Crystal system	orthorhombic	
Space group	Pca21	
a (Å)	16.7226(5)	16.8792(4)
b (Å)	6.1425(2)	6.25550(10)
c (Å)	15.6940(4)	15.4458(3)
α (°)	90	90
β (°)	90	90
γ (°)	90	90
V (Å ³)	1612.07(8)	1630.89(6)
Z	4	4
D _{calc} (Mg/m ³)	1.620	1.628
Absorption coefficient (mm ⁻¹)	1.102	1.543
F(000)	812	824
Crystal size (mm ³)	0.330 × 0.102 × 0.085	0.240 × 0.134 × 0.134
Theta range for data collection (°)	2.436–26.373	2.413–30.456
Index ranges	−20 ≤ h ≤ 20, −7 ≤ k ≤ 7, −19 ≤ l ≤ 19	−24 ≤ h ≤ 24, −8 ≤ k ≤ 8, −21 ≤ l ≤ 20
Reflections collected	15 133	15 241
Independent reflections	3295 [R _{int} = 0.0216]	4645 [R _{int} = 0.0198]
Refinement method	full-matrix least-squares on F ²	
Data/restraints/parameters	3295/4/240	4645/7/240
Goodness-of-fit on F ²	1.051	1.023
Final R indices [I > 2σ(I)]	R ₁ = 0.0169, wR ₂ = 0.0445	R ₁ = 0.0188, wR ₂ = 0.0464
R indices (all data)	R ₁ = 0.0171, wR ₂ = 0.0446	R ₁ = 0.0199, wR ₂ = 0.0468

yielded dark-magenta and transparent crystals, respectively. These crystals, which are insoluble in common solvents and appear to be air and moisture stable, correspond to the novel compounds **1** and **2**, respectively. These are unique examples of complexes, with mixed innocent bi-dentate (fum and dbpy) and mono-dentate (aqua) ligands, having distorted trigonal-prismatic geometry around the hexa-coordinated metal ions, which classifies them as metaprisms [7].

3.2. Description of structures for Co(II)(H₂O)₂(dbpy)(fum) (**1**) and Zn(II)(H₂O)₂(dbpy)(fum) (**2**)

Complexes **1** and **2** crystallize in orthorhombic space group Pca21. These complexes can be considered isostructural, although subtle differences emerge in their distorted trigonal-prismatic geometries (*vide infra*). A perspective view of the complexes with selected atom-numbering scheme is shown in Fig. 1. Selected bond distances, bond angles and hydrogen bonding geometries of **1** and **2** are listed in Tables 2 and 3, respectively. In both complexes, the metal ion is hexa-coordinated with a N₂O₄ distorted trigonal-prismatic coordination environment, with one fum ligand, one dbpy ligand and two coordinated water molecules. The metal to nitrogen distances are 2.1448(18) and 2.1216(18) Å for **1**, and 2.1573(14) and 2.1228(14) Å for **2**. The metal to oxygen distances for the fum ligand for each M–O bond are almost the same; they are 2.1103(16) and 2.3041(15) for **1**, and 2.0349(14) and 2.5655(14) for **2**. The two M–O bonds for coordinated water molecules are 2.0603(16) and 2.0437(17) for **1**, and 2.0728(13) and 2.0363(13) for **2**. The bite angles for the fum ligand are 59.27(6)° and 55.75(5)° for **1** and **2**, respectively. The dbpy ligand has a bite angle of 75.59(7)° and 76.33(6)° for **1** and **2**, respectively. The fum ligand is almost planar in **2**, with an angle of 1.63° between the least-squares planes of the two carboxylates, **1** has a more twisted fum ligand with an angle of 6.39°; the angles between the least-squares planes through the rings of the dbpy ligand are 8.50° and 10.07° for **1** and **2**, respectively, and this ligand is thus not planar in both complexes. The obtuse angles between the least-squares mean planes of the chelate rings, and the plane of the two water molecules and the metal, lie in the range 108.93–133.99° for **1** and 108.66–135.08° for **2**, in concordance with a distorted trigonal-prismatic coordination geometry.

The two trigonal-faces of the metaprisms are constituted by one oxygen atom of the fum ligand, one nitrogen atom from the dbpy ligand and one oxygen atom from a water molecule. Figs. 1b and 2b show the distorted trigonal-prismatic coordination geometry around Co(II) and Zn(II), respectively, in more detail. For **1**, the lengths of the triangular sides are in the range 2.953–2.962 Å for the triangle O1–N1–O6 and 2.992–3.041 Å for the triangle O2–N2–O7, all angles are in the range 58.97–60.56°. The two fum oxygen atoms and the two oxygen atoms from two aqua ligands make up a trapezoid, which should be a perfect square for ideal trigonal-

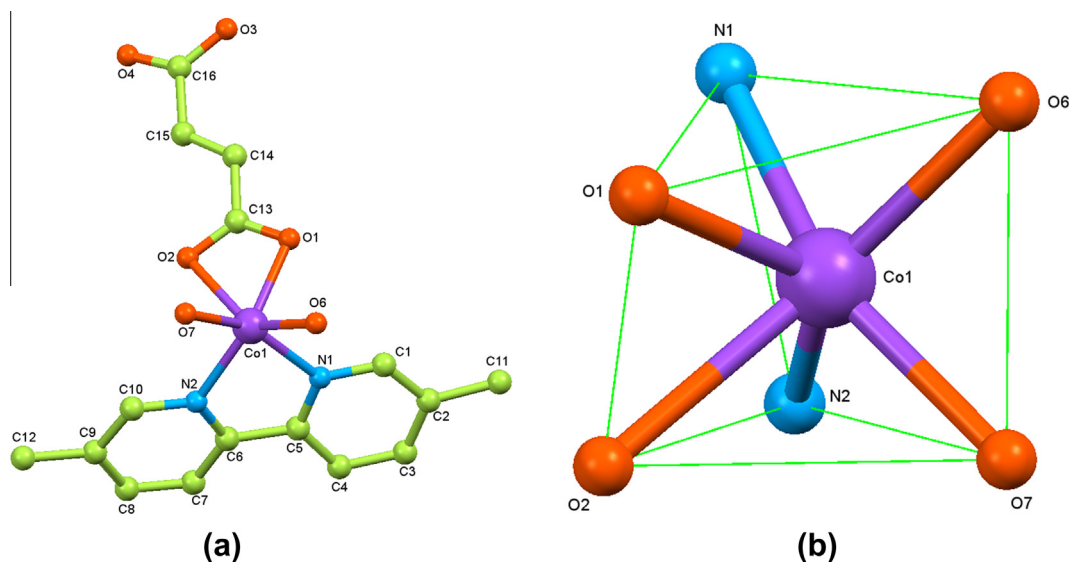


Fig. 1. Molecular structure of Co(H₂O)₂(dbpy)(fum) (**1**) (a); detail of distorted trigonal-prismatic coordination geometry of **1** (b).

Table 2
Selected bond distances (Å) and angles (°) for **1**.

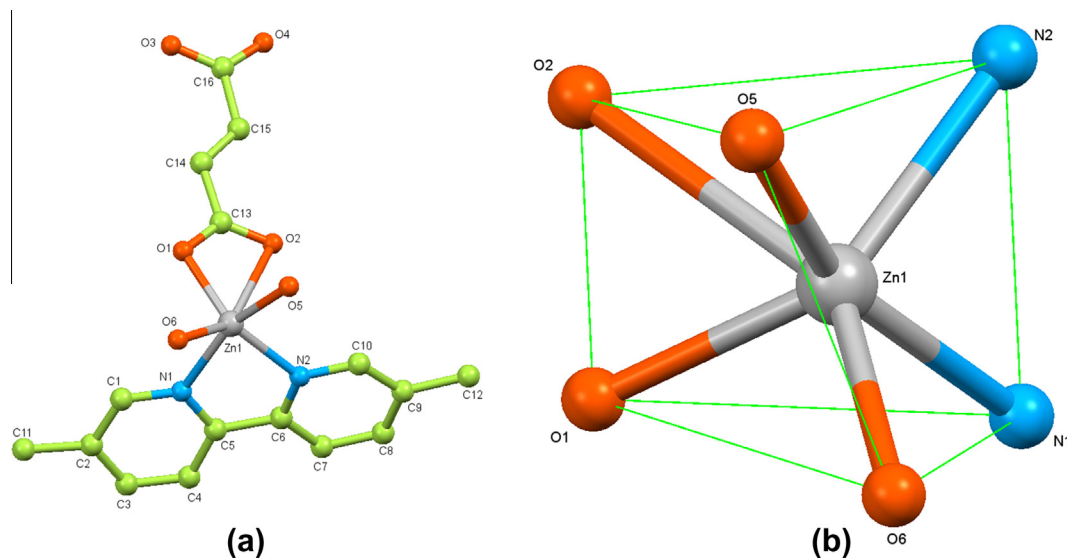
Bond lengths (Å)				
Co(1)–O(7)	2.0437(17)	Co(1)–N(2)	2.1216(18)	
Co(1)–O(6)	2.0603(16)	Co(1)–N(1)	2.1448(18)	
Co(1)–O(1)	2.1103(16)	Co(1)–O(2)	2.3041(15)	
Angles (°)				
O(7)–Co(1)–O(6)	82.22(6)	O(1)–Co(1)–N(1)	87.87(7)	
O(7)–Co(1)–O(1)	114.81(8)	N(2)–Co(1)–N(1)	75.59(7)	
O(6)–Co(1)–O(1)	90.45(6)	O(7)–Co(1)–O(2)	88.56(6)	
O(7)–Co(1)–N(2)	93.66(7)	O(6)–Co(1)–O(2)	140.80(6)	
O(6)–Co(1)–N(2)	133.41(7)	O(1)–Co(1)–O(2)	59.27(6)	
O(1)–Co(1)–N(2)	131.68(7)	N(2)–Co(1)–O(2)	84.97(6)	
O(7)–Co(1)–N(1)	155.76(7)	N(1)–Co(1)–O(2)	111.58(6)	
O(6)–Co(1)–N(1)	89.51(7)			
D–H...A				
O(6)–H(6A)...O(3)#1	0.838(12)	1.856(14)	2.678(2)	166(3)
O(6)–H(6B)...O(2)#2	0.836(17)	1.862(17)	2.692(2)	171(3)
O(7)–H(7A)...O(4)#1	0.85(2)	1.77(2)	2.620(2)	170(3)
O(7)–H(7B)...O(3)#3	0.85(2)	1.84(2)	2.685(2)	179(3)

Symmetry transformations used to generate equivalent atoms.

#1 $-x+3/2, y+1, z-1/2$; #2 $x, y+1, z$; #3 $-x+3/2, y, z-1/2$.**Table 3**
Selected bond distances (Å) and angles (°) for **2**.

Bond lengths (Å)				
Zn(1)–O(1)	2.0349(14)	Zn(1)–N(2)	2.1228(14)	
Zn(1)–O(6)	2.0363(13)	Zn(1)–N(1)	2.1573(14)	
Zn(1)–O(5)	2.0728(13)	Zn(1)–O(2)	2.5655(14)	
Angles (°)				
O(1)–Zn(1)–O(6)	95.82(6)	O(5)–Zn(1)–N(1)	159.37(6)	
O(1)–Zn(1)–O(5)	103.59(7)	N(2)–Zn(1)–N(1)	76.33(6)	
O(6)–Zn(1)–O(5)	83.10(5)	O(1)–Zn(1)–O(2)	55.75(5)	
O(1)–Zn(1)–N(2)	131.53(6)	O(6)–Zn(1)–O(2)	146.07(5)	
O(6)–Zn(1)–N(2)	131.40(6)	O(5)–Zn(1)–O(2)	86.21(5)	
O(5)–Zn(1)–N(2)	93.76(6)	N(2)–Zn(1)–O(2)	81.28(5)	
O(1)–Zn(1)–N(1)	96.41(6)	N(1)–Zn(1)–O(2)	109.61(5)	
O(6)–Zn(1)–N(1)	89.95(6)			
D–H...A				
O(5)–H(5A)...O(4)#1	0.845(18)	1.81(2)	2.6454(19)	168(2)
O(5)–H(5B)...O(3)#2	0.801(18)	1.925(18)	2.7200(17)	171(2)
O(6)–H(6A)...O(3)#1	0.799(19)	1.88(2)	2.6651(19)	166(2)
O(6)–H(6B)...O(2)#3	0.854(19)	1.802(19)	2.650(2)	171(2)

Symmetry transformations used to generate equivalent atoms.

#1 $-x+1/2, y+1, z-1/2$; #2 $-x+1/2, y, z-1/2$; #3 $x, y+1, z$.**Fig. 2.** Molecular structure of $\text{Zn}(\text{H}_2\text{O})_2(\text{dbpy})(\text{fum})$ (**2**) (a); detail of distorted trigonal-prismatic coordination geometry of **2** (b).

prismatic geometry, the sides of which are in the range of 2.189–3.041 Å. The remaining two faces of the prism are also trapezoids consisting of two oxygen atoms of the fum ligand and two oxygen atoms of the aqua ligands, which are joined by the two nitrogen atoms of the dbpy ligand, respectively. Both faces have an O–O distance of 2.189 and 2.698 Å, an N–O distance in the range 2.953–3.038 Å, and a distance of 2.614 Å for the N1–N2 side. Due to these markedly differences in distances of the trapezoid faces of the prism, the two triangular faces are not parallel. Thus, the planes defined by O1–N1–O6 and O2–N2–O7 make an angle of 21.52°. The torsion angles about the centroids of the triangular faces and each of the corners (i.e., Ct1–N1–N2–Ct2) are 14.14°, 15.88° and 14.80°. Likewise, for **2** the lengths of the triangular sides are in the range 2.965–3.127 Å for the triangle O1–N1–O6 and 3.063–3.190 Å for the triangle O2–N2–O5, all angles are in the range 57.65–62.96°. The two fum oxygen atoms and the two oxygen atoms from two aqua ligands make up a trapezoid, the sides of which are in the range of 2.201–3.190 Å. The remaining two sides of the prism are also trapezoids consisting of two oxygen atoms of the fum ligand and two oxygen atoms of the aqua ligands, which are joined by the two nitrogen atoms of the dbpy ligand, respectively. Both faces have an O–O distance of 2.201 and 2.725 Å, an N–O distance in the range 2.965–3.127 Å, and a distance of 2.645 Å for the N1–N2 side. Therefore, the planes defined by O1–N1–O6 and O2–N2–O5 make an angle of 24.62°. The torsion angles about the centroids of the triangular faces and each of the corners are -18.47 , -26.67 and -16.83° . A perfect trigonal prism would have angles of 0° , the triangular faces precisely overlapping.

Complexes and coordination polymers including dicarboxylate ligands with one carboxylate end coordinated and the other end uncoordinated, this is, as a carboxylate anion, have been reported [23]. There are also complexes where fumarate di-anion is acting as a counter-ion [24]. However, complexes specifically bearing a fumarate ligand with one end coordinated to a metal ion and the other carboxylate end of the ligand remaining uncoordinated are definitely rare or non-existing. Therefore, it seems that complexes **1** and **2** are the first mononuclear coordination complexes obtained possessing a dicarboxylate fumarate ligand with a unique chelating (bidentate, $\eta^1:\eta^1$) non-bridging coordination mode [25]. The existence of this unusual coordination mode for a dicarboxylate ligand in **1** and **2** is clearly motivated by the intermolecular hydrogen-bonding interactions occurring in these complexes (*vide infra*).

Several years ago it was said that the most important factors for controlling the coordination geometry were, the ligand structural constraints (including the rigidity of the ligand framework and intra-ligand repulsions), ligand field stabilization energy (LFSE) considerations, possible ligand–metal π -backbonding effects and the size of the metal ion [26]. Nevertheless, nowadays it could be said that even the possibility of an extended structure, polymeric or supramolecular in nature, along with the solid-state crystal packing, could influence the expected coordination geometry in a complex.

Complexes **1** and **2** exhibit intermolecular interactions due to hydrogen bonding. These interactions are promoted by the presence of the aqua ligands and the non-coordinated oxygen atoms of the fum carboxylate. These conditions can be clearly observed for **1** in Fig. 3a, where the main O–H–O bindings are formed by the O–H moieties of each aqua ligand with each of the oxygen atoms of the non-coordinated side of one fum ligand, generating,

thus, a central chain. Moreover, each coordinated water molecule generates a double hydrogen bridge, the one that is already described above, and other with one fum oxygen atom already coordinated to Co(II) of a neighboring molecule. Since both coordinated water molecules perform this kind of connectivity, an extended 2D supramolecular structure is generated (Fig. 3). Almost identical intermolecular bonding conditions occur for **2** (Fig. 4), producing also a very stable 2D supramolecular array in the solid-state. The structural characteristics, both molecular and supramolecular, and the stability of **1** and **2**, could also be influenced by the presence of π – π interactions in the dbpy ligands, as depicted for complex **2** in Fig. 4a, which appear in both extended systems obtained. The distances between these π – π stacking interactions of the dbpy rings are 3.755 and 3.831 Å for **1** and **2**, respectively.

A plausible explanation for complexes **1** and **2** to adopt such a distinctive coordination geometry, could come precisely from their

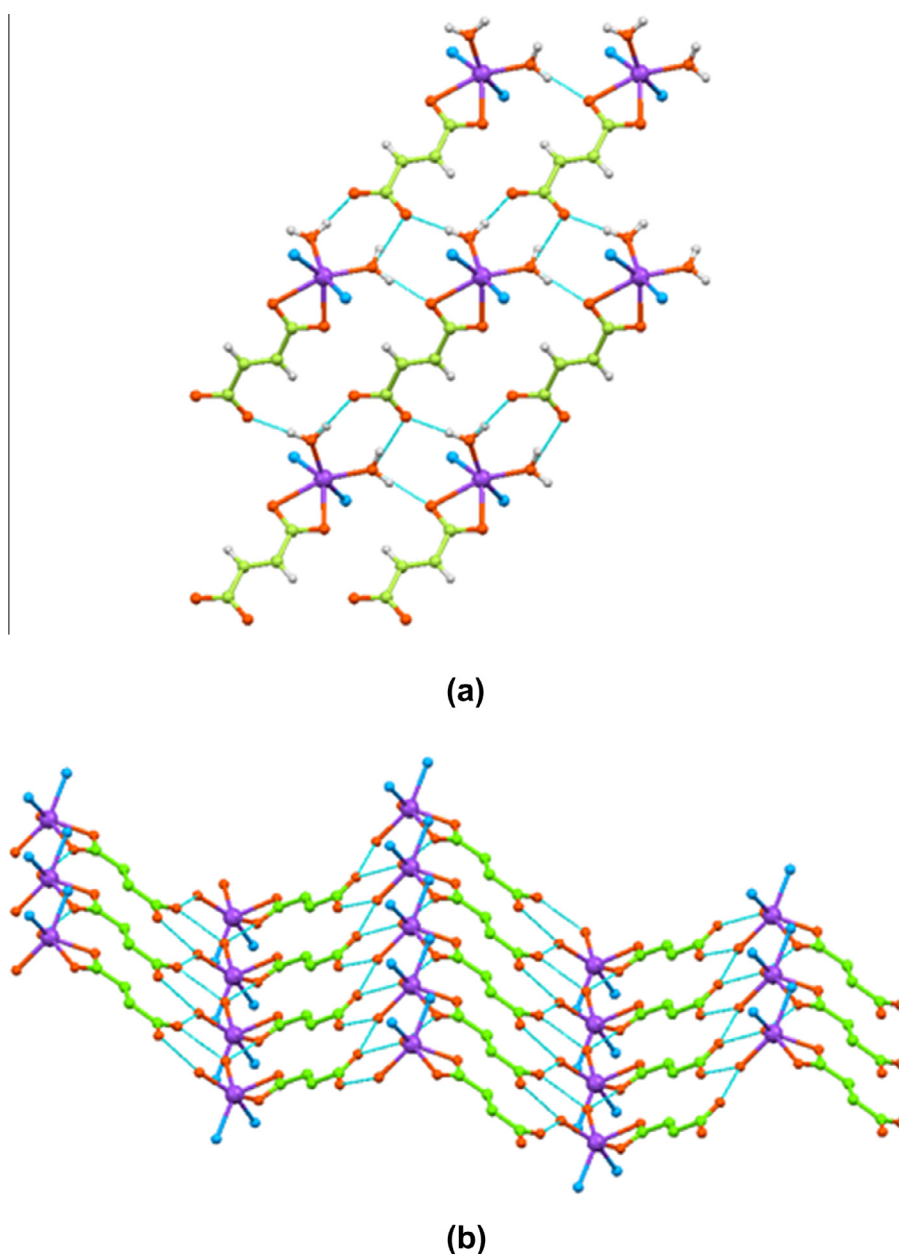


Fig. 3. Hydrogen bonding main connections in **1**, view looking down *a* axis; carbon-skeleton of dbpy is omitted for clarity (a). 2D supramolecular wrinkle-sheet type structure of **1**, view looking down almost *b* axis; hydrogens and carbon-skeleton of dbpy are omitted for clarity (b).

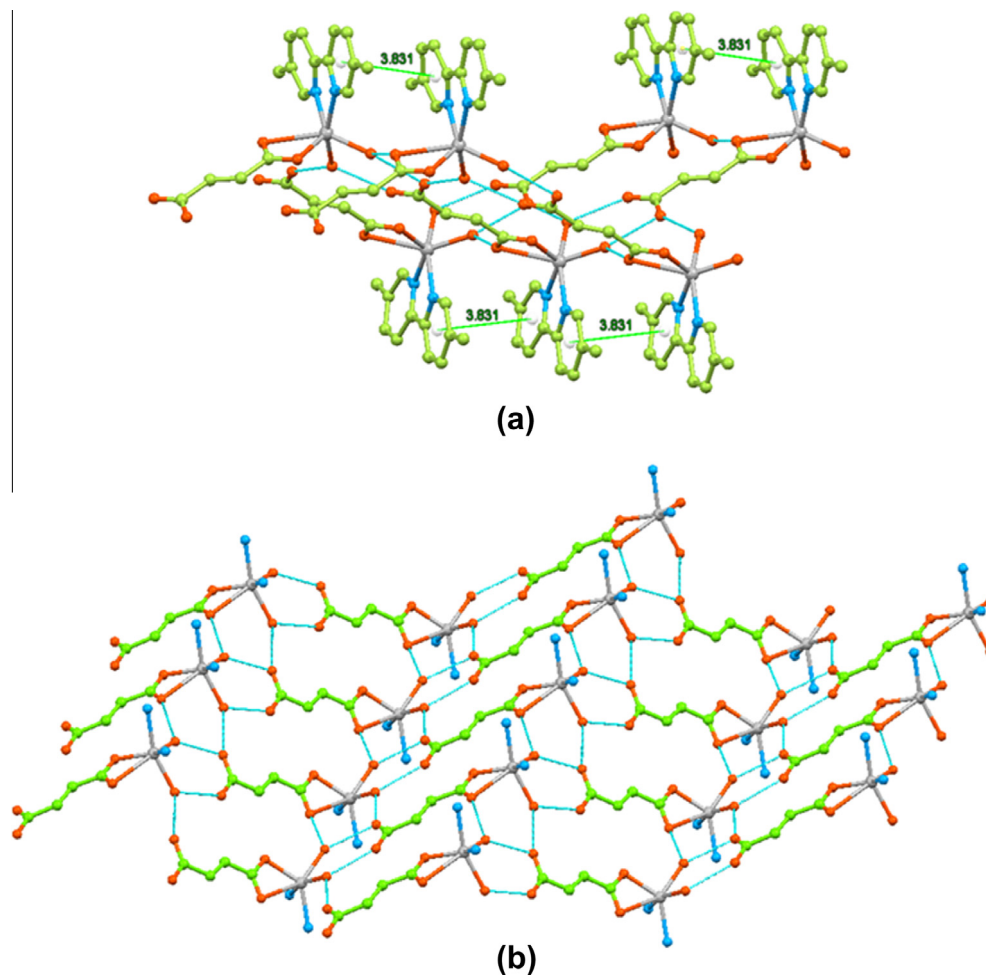


Fig. 4. Hydrogen bonding main connections and π - π interactions in **2**, view looking down almost *c* axis; hydrogens are omitted for clarity (a). 2D supramolecular wrinkle-sheet type structure of **2**, view looking down almost *b* axis; hydrogens and carbon-skeleton of dbpy ligand are omitted for clarity (b).

supramolecular arrays. If one looks closely the hydrogen-bridging motif in Fig. 3a, both coordinated water molecules are attached by three bindings, one with the metal ion, and two by forming hydrogen interactions with fum carboxylate oxygen atoms. These connections lead to the formation of “quasi-chelate” coordination mode for the aqua ligands around the Co(II) ions, generating two different types of fused eight-members rings, additionally connected to larger rings (Fig. 3a). The eight-member rings where the two aqua ligands of a same molecule are involved, include, besides de metal ion, two oxygen atoms and two hydrogen atoms from the aqua ligands, two oxygen atoms from the uncoordinated carboxylate of fum and a carbon atom of the carboxylate group also from the fum ligand. These structural conditions, that occur in both complexes, can preclude larger bite angles for the fum carboxylates and for the aqua ligands to bind the metal ion in a different or larger angle, provoking thus the preference of **1** and **2** for a distorted trigonal-prismatic coordination geometry rather than the more conventional octahedral one, and, as a consequence, formation of supramolecular structures with stable crystal packing in the solid-state. Cases where π -backbonding effects, crystal packing, and rigidity of ligands influence the structure of complexes acquiring the trigonal prismatic geometry have been reported [26,27]. Some relatively recent examples of Co(II) and Zn(II) complexes possessing a distorted trigonal-prismatic have been reported [28,29]. Nonetheless, to our knowledge complexes **1** and **2** are the first cases where the preference of distorted trigonal-prismatic

over the typical octahedral coordination geometry may be dictated by supramolecular interactions.

3.3. Thermal analyses

To examine the thermal stability of the complexes, thermal analyses were performed for **1** and **2** between 20 and 800 °C (Supplementary data).

Complexes **1** and **2** exhibit mainly three decomposition stages. The first major weight loss (10.00%) for **1** occurs between 120 and 160 °C, the second one, with a weight loss of 60.43% of the initial weight, takes place approximately between 250 and 380 °C. The last weight loss occurs at 390 °C where only 18% of the initial sample weight remains at 800 °C. Likewise, for **2** the first weight loss (~8%) appears between 65 and 250 °C, the second one, with a weight loss of 59.59%, happens between 342 and 415 °C, and the third one occurs at 435 °C, leaving around 35% of the initial sample weight at 800 °C. In both complexes, the first decomposition stage can be endorsed to the loss of coordinated water, although in complex **2** its initial thermal behavior shows also presence of non-coordinated water in the sample; the rest of the stages can be attributed practically to the combined weight loss of the fum (Calc. 29.00% for **1** and 28.53% for **2**) and dbpy (Calc. 46.85% for **1** and 46.09% for **2**) ligands. The residual of the initial weight loss, at 800 °C, can be assigned to CoO (Calc. 19.00%) for **1**. However, in complex **2** it seems that the thermal degradation at 800 °C was

not enough in order to remove all ligands to attain residual ZnO (Calc. 20.36%).

3.4. Magnetic properties of **1**

The calculated magnetic susceptibility (χ), in terms of cm^3/mol , versus temperature for **1**, can be seen in Fig. 5a; whereas, the inverse susceptibility (χ^{-1}) versus temperature plot was fitted to a simple Curie model (Fig. 5b). Magnetic susceptibility of **1** was determined at zero field cooling (ZFC) and field cooling (FC) from 2 to 300 K and decreasing (Fig. 5a). This measurements protocol revealed a hysteresis, observed mainly in the χ^{-1} versus T plot (Fig. 5b). The Curie constant was determined to be $2.87 \text{ cm}^3 \text{ K/mol}$, $S = 3/2$, with a small orbital contribution, not totally quenched and influences to a value of orbital angular contribution less than one. The Curie–Weiss temperature was determined to be $\theta_{(C-W)} = -14 \text{ K}$, indicative of an antiferromagnetic ordering. The low temperature decreasing of χ^{-1} could be caused by weak intermolecular antiferromagnetic exchange because zero-field splitting of the $^4T_{1g}$ ground state [30]. Regularly, the effects of spin–orbit coupling occur in combination with the effects of a symmetry-lowering structural distortion, for instance away from O_h symmetry [31], as it is the case for complex **1**. From the χT value obtained at

300 K, a $\mu_{\text{eff}} = 4.67 \mu_B$ is calculated, which is higher than the expected spin-only value of $3.87 \mu_B$ corresponding to three unpaired electrons for high-spin $d^7\text{-Co}^{2+}$; however, the obtained value agrees with those reported in literature for high-spin Co(II) complexes [32] and also confirms an $S = 3/2$ spin state. These results are in concordance with a previous magnetic study carried out on a Co(II) complex having distorted trigonal-prismatic geometry [33]. It is supposed that this type of coordination sphere promotes the removal of the orbital degeneracy, which usually occurs in Co(II) octahedral complexes and, as a consequence, these systems may be described as an effective Co(II) spin of $3/2$ with a moderate anisotropy. Nonetheless, it was difficult to fit the Curie–Weiss model to the χT versus T plot particularly below 25 K (Supplementary data). Therefore, assuming that in the low-temperature region the spin–orbit coupling is promoted in this system, the magnetic exchange interactions and the spin–orbit coupling for complex **1** were also estimated based on the simple phenomenological equation $\chi T = A_{\text{exp}}(-E_1/kT) + B_{\text{exp}}(-E_2/kT)$, where $A + B$ is equal to the Curie constant and E_1 and E_2 are the “activation energies” of the spin–orbit coupling and the magnetic interaction, respectively [34]. As shown in Fig. 6, for the χT versus T plot, Rueff model follows very well the experimental data, even at the lowest temperature studied. The best parameters obtained with the Rueff procedure after least-squares fitting are $A + B = 2.88 \text{ emu K mol}^{-1}$, which perfectly agrees with values given in the literature for the Curie constant ($C = 2.8\text{--}3.5 \text{ emu K mol}^{-1}$), and also practically equals the value obtained from the fitting of Curie–Weiss model showed previously. The effect of the spin–orbit coupling $E_1 = 32.65 \text{ cm}^{-1}$ is lower than values reported for other Co(II) systems ($\sim 50 \text{ cm}^{-1}$) [34,35], which, by the way, they are not supramolecular systems but rather are extended coordinated compounds. The positive, and low, value of activation energy $E_2 = 0.24 \text{ cm}^{-1}$ confirms both, that antiferromagnetic exchanges are effective in complex **1** and that these interactions are weak.

It is noteworthy to mention that, presumably, the main magnetic exchange pathway appears to be the strong hydrogen binding interactions occurring through the connections involving the coordinated water (O6) and one of the oxygen atoms (O2) in the carboxylate moiety of fum ligand, belonging to a neighboring complex molecule, [Co–O6–H6B–O2–Co] (Fig. 3). These interactions, alongside to the π – π stacking non-bonding contacts of dbpy rings, produces the shortest Co–Co distance of 6.143 \AA in the supramolecular structure of **1**.

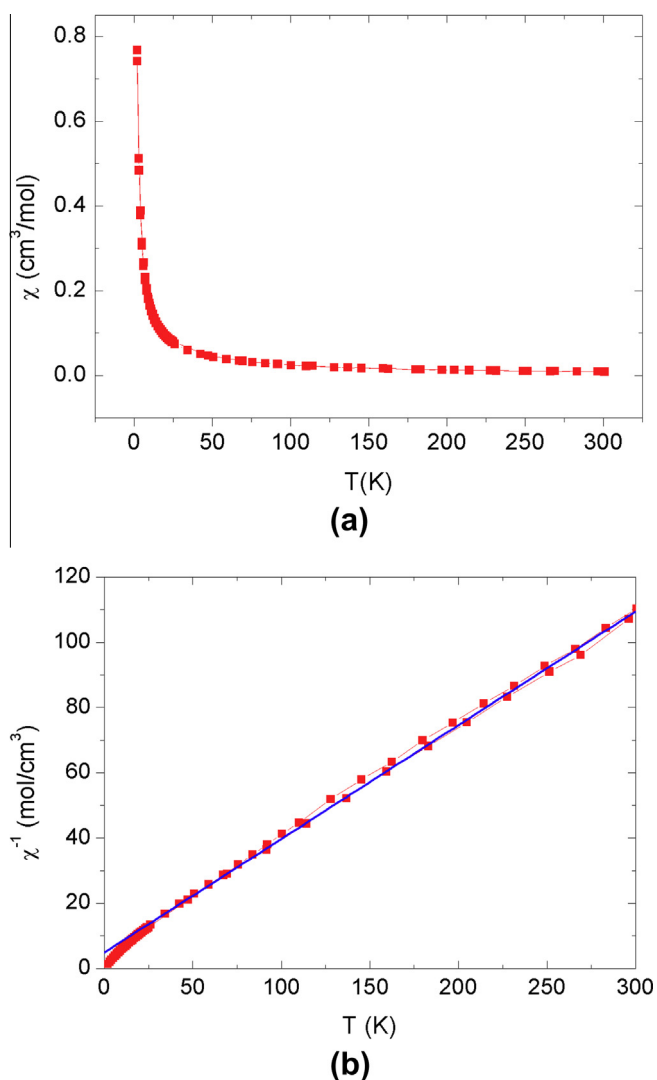


Fig. 5. χ vs T plot (a) and χ^{-1} vs T plot (b) for **1**. Blue line corresponds to Curie–Weiss model fitting (b). (Color online.)

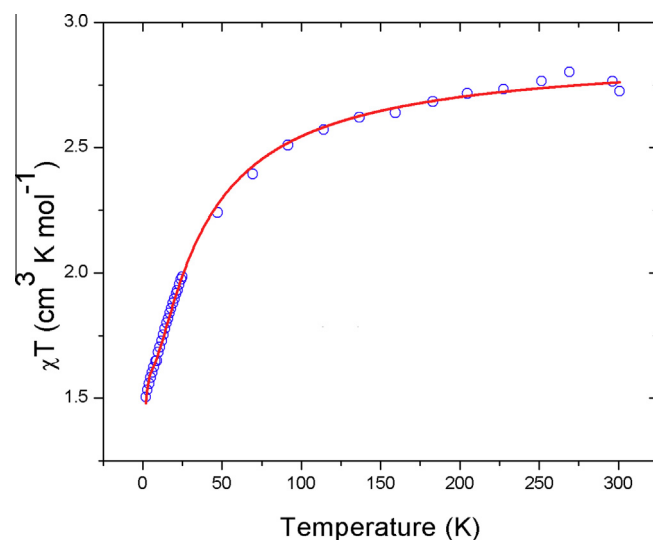


Fig. 6. χT vs T plot for **1**. Red line corresponds to Rueff phenomenological model fitting. (Color online.)

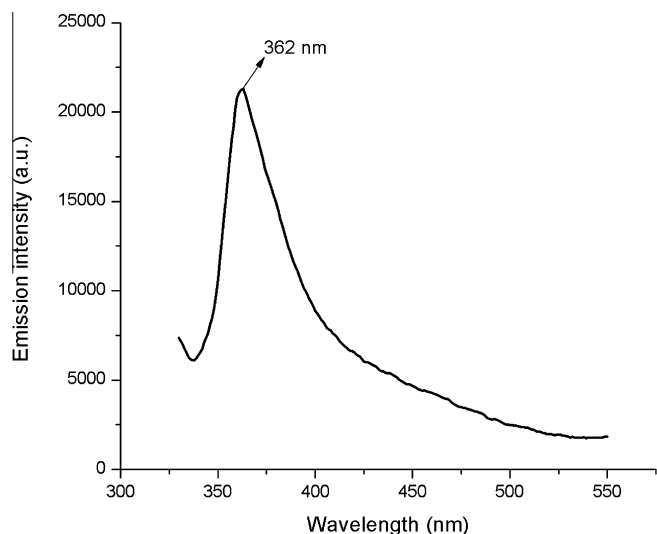


Fig. 7. Fluorescent emission spectrum of **2** in solid-state at room temperature. $\lambda_{\text{exc}} = 310$ nm.

3.5. Photoluminescence properties of **2**

As shown in Fig. 7, compound **2** display a strong blue photoluminescence emission band in the solid-state, with the emission maximum at 362 nm upon excitation at 310 nm. This band seem to proceed from the intraligand ($\pi-\pi^*$) fluorescent emission since Zn(II) ion is difficult to oxidize or to reduce due to its d^{10} configuration [36]. Thus, this emission seems to be neither metal-to-ligand (MLCT) nor ligand-to-metal charge transfer in nature [37]. Numerous aromatic ligands, such as dbpy, possess some degree of fluorescence, which is usually enhanced when coordinated to Zn(II). This enhancement can be the result of the actual coordination of these types of ligands to the metal ion, situation that strengthens their conformational rigidity and minimizes the non-radiative decay of the intraligand ($\pi-\pi^*$) excited states [38]. Similar explanation for the photoluminescence properties of Zn(II) complexes has been reported before [39]. In addition, the photoluminescence properties of **2** could also be related to the ligand rigidity effect caused by the formation of the 2D supramolecular array in the solid-state, which, as mentioned above, may generate its unusual coordination geometry.

4. Conclusions

We have demonstrated the synthesis, using simple one-pot solution reactions, and the structural characterization of uncommon Co(II) and Zn(II) distorted trigonal-prismatic complexes having innocent bi-dentate ligands and, in particular, aqua ligands in their coordination sphere. Moreover, the $\eta^1:\eta^1$ non-bridging coordination mode of fumarato ligand appears for the first time in these type of mononuclear complexes. It seems that these complexes owe their rare coordination geometry to the extended structure generated in the solid-state, due primarily to intermolecular hydrogen-bonding interactions between the aqua ligands and the non-coordinated oxygen atoms from the fumarato ligand, resulting in 2D arrays. Therefore, compounds **1** and **2** are the first examples of metaprisms with aqua ligands in their coordination spheres, and also the first complexes reported where the distorted trigonal-prismatic geometry is presumably acquired due to the supramolecular interactions determining the final solid-state structure. Complex **1** exhibits weak antiferromagnetic coupling characteristic of a Co(II) high-spin complex in a distorted

trigonal-prismatic geometry; meanwhile, complex **2** might be a good blue-light emitting material in the solid-state.

Acknowledgments

Funding for this work was provided by Universidad Autónoma del Estado de México through research project 3584/2013CHT. Authors are indebted to Dr. Diego Martínez-Otero (CCIQS UAEM-UNAM) for single-crystal X-ray diffraction studies, to Dra. Susana Hernández-López (LIDMA-FQ-UAEM) for TGA analyses and to M. en C. Alejandra Nuñez (CCIQS UAEM-UNAM) for elemental analyses. This work was also supported by CONACYT project 129293, DGAPA-UNAM project IN106014, and ICyTDF, project PICCO. We thank to Dr. Francisco Morales Leal (IIM-UNAM) for assistance in magnetic properties models fitting. R.E. thanks to J. Morales and A. Lopez (IIM-UNAM), for help in computational and technical problems, and to F. Silvar (IIM-UNAM) for He provisions.

Appendix A. Supplementary data

CCDC 1013316 and 1059991 contains the supplementary crystallographic data for **1** and **2**, respectively. These data can be obtained free of charge via <http://www.ccdc.cam.ac.uk/conts/retrieving.html>, or from the Cambridge Crystallographic Data Centre, 12 Union Road, Cambridge CB2 1EZ, UK. Fax: +44 1223-336-033; or e-mail: deposit@ccdc.cam.ac.uk.

Supplementary data associated with this article can be found, in the online version, at <http://dx.doi.org/10.1016/j.poly.2015.08.025>.

References

- [1] S.G. Sreerama, S. Pal, *Inorg. Chem. Commun.* 4 (2001) 656.
- [2] E. Larsen, G.N. Lamar, B.E. Wagner, R.H. Holm, J.E. Parks, *Inorg. Chem.* 11 (1972) 2652.
- [3] R.A.D. Wentworth, *Coord. Chem. Rev.* 9 (1972) 171.
- [4] M.F. Lappert, C.L. Raston, B.W. Skelton, A.H. White, *J. Chem. Soc., Chem. Commun.* (1981) 485.
- [5] P.M. Morse, G.S. Girolami, *J. Am. Chem. Soc.* 111 (1989) 4114.
- [6] J.C. Friese, A. Krol, C. Puke, K. Kirschbaum, D.M. Giolando, *Inorg. Chem.* 39 (2000) 1496.
- [7] E. Cremades, J. Echeverría, S. Alvarez, *Chem. Eur. J.* 16 (2010) 10380.
- [8] M.J. Roma, *Dalton Trans.* (2009) 4053.
- [9] H.S. Rzepa, M.E. Cass, *Inorg. Chem.* 46 (2007) 8024.
- [10] M. Dua, C.-P. Li, C.-S. Liub, S.-M. Fang, *Coord. Chem. Rev.* 257 (2013) 1282.
- [11] D. Curiel, M. Más-Montoya, G. Sánchez, *Coord. Chem. Rev.* 284 (2014) 19.
- [12] (a) Y.-Q. Zheng, J.-L. Lin, B.-Y. Chen, *J. Mol. Struct.* 646 (2003) 151; (b) J.W. Sprengers, M.J. Agerbeek, C.J. Elsevier, H. Kooijman, A.L. Spek, *Organometallics* 23 (2004) 3117; (c) M. Devereux, M. McCann, V. Leon, M. Geraghty, V. McKee, J. Wikaira, *Polyhedron* 19 (2000) 1205.
- [13] (a) S.J. Bora, B.K. Das, *J. Solid State Chem.* 192 (2012) 93; (b) G. Yang, Z.-H. Sun, *Inorg. Chem. Commun.* 29 (2013) 94; (c) Z. Shi, L. Zhang, S. Gao, G. Yang, J. Hua, L. Gao, S. Feng, *Inorg. Chem.* 39 (2000) 1990; (d) C. Gabriel, C.P. Raptopoulou, V. Psycharis, A. Terzis, M. Zervou, C. Mateescu, A. Salifoglou, *Cryst. Growth Des.* 11 (2011) 382.
- [14] B.O. Patrick, W.M. Reiff, V. Sanchez, A. Storr, R.C. Thompson, *Inorg. Chem.* 43 (2004) 2330.
- [15] R.D. Hancock, *Chem. Soc. Rev.* 42 (2013) 1500.
- [16] J.M. Lehn, *Supramolecular Chemistry*, VCH, Weinheim, 1995.
- [17] G.R. Desiraju, J.J. Vittal, A. Ramanan, *Crystal Engineering-A Text Book*, IISc Press and World Scientific, Singapore, 2011.
- [18] A.D. Burrows, C.G. Frost, M.F. Mahon, P.R. Raithby, C.L. Renouf, C. Richardson, A.J. Stevenson, *Chem. Commun.* 46 (2010) 5067.
- [19] X.H. Zhou, L. Li, H.H. Li, A. Li, T. Yang, W. Huang, *Dalton Trans.* 42 (2013) 12403.
- [20] APEX 2 Software Suite. Bruker AXS Inc., Madison, Wisconsin, USA.
- [21] G.M. Sheldrick, *Acta Crystallogr., Sect. A* 64 (2008) 112.
- [22] C.B. Hübschle, G.M. Sheldrick, B. Dittrich, *J. Appl. Crystallogr.* 44 (2011) 1281.
- [23] Bigyan R. Jali, Jubaraj B. Baruah, *Inorg. Chem. Commun.* 14 (2011) 1440.
- [24] (a) M. Padmanabhan, J.C. Joseph, X. Huang, J. Li, *J. Mol. Struct.* 885 (2008) 36; (b) J.C. Kim, A.J. Lough, H. Park, Y.C. Kang, *Inorg. Chem. Commun.* 9 (2006) 514.
- [25] (a) F.A. Mautner, R. Vicente, F.R.Y. Louka, S.S. Massoud, *Inorg. Chim. Acta* 361 (2008) 1339; (b) Y.-Z. Zhenga, Z. Zhenga, X.-M. Chen, *Coord. Chem. Rev.* 258–259 (2014) 1; (c) J. Do, Y. Lee, J. Kang, A.J. Jacobson, *Inorg. Chim. Acta* 382 (2012) 191;

- (d) L. Canadillas-Delgado, O. Fabelo, J. Cano, J. Pasan, F.S. Delgado, F. Lloret, M. Julve, C. Ruiz-Perez, *Cryst. Eng. Comm.* 11 (2009) 2131.
- [26] S.A. Kubow, K.J. Takeuchi, J.J. Grzybowski, A.J. Jircitano, V.L. Goedken, *Inorg. Chim. Acta* 241 (1996) 21.
- [27] R. van Gorkum, F. Buda, H. Kooijman, A.L. Spek, E. Bouwman, J. Reedijk, *Eur. J. Inorg. Chem.* (2005) 2255.
- [28] (a) C.P. Pradeep, P.S. Zacharias, S.K. Das, *Eur. J. Inorg. Chem.* (2007) 5377;
(b) Y.Z. Voloshin, O.A. Varzatskii, A.S. Belov, A.V. Vologzhanina, Z.A. Starikova, A.V. Dolganov, V.V. Novikov, *Inorg. Chim. Acta* 362 (2009) 5144;
(c) Y.Z. Voloshin, O.A. Varzatskii, A.S. Belov, Z.A. Starikova, A.V. Dolganov, V.V. Novikov, Y.N. Bubnov, *Inorg. Chim. Acta* 370 (2011) 322;
(d) M.P. Bubnov, N.A. Skorodumova, E.V. Baranov, A.S. Bogomyakov, A.V. Arapova, N.N. Smirnova, V.K. Cherkasov, G.A. Abakumov, *Inorg. Chim. Acta* 392 (2012) 84;
(e) Y.Z. Voloshin, A.Y. Lebedev, V.V. Novikov, A.V. Dolganov, A.V. Vologzhanina, E.G. Lebed, A.A. Pavlov, Z.A. Starikova, M.I. Buzin, Y.N. Bubnov, *Inorg. Chim. Acta* 399 (2013) 67;
(f) S. Tsiliou, L.-A. Kefala, F. Perdih, I. Turel, D.P. Kessissoglou, G. Psomas, *Eur. J. Med. Chem.* 48 (2012) 132;
(g) I. Karthikeyan, S.K. Alamsetti, G. Sekar, *Organometallics* 33 (2014) 1665.
- [29] (a) J.C. Knight, R. Prabakaran, A.J. Amoroso, P.G. Edwards, L.-I. Ooi, *Polyhedron* 31 (2012) 457;
(b) A.M. Najjar, C. Avci, M.D. Ward, *Inorg. Chem. Commun.* 15 (2012) 126;
(c) A.M.T. Bygott, R.J. Geue, S.F. Ralph, A.M. Sargeson, A.C. Willis, *Dalton Trans.* (2007) 4778;
(d) C. Lampe-Onnerud, H.-C. zur Loye, *Inorg. Chem.* 35 (1996) 2155.
- [30] M. Murrie, *Chem. Soc. Rev.* 39 (2010) 1986.
- [31] O. Kahn, *Molecular Magnetism*, VCH Publishers, New York, 1993.
- [32] R.L. Carlin, *Magnetochemistry*, Springer-Verlag, Berlin, 1986.
- [33] N.A. Protasenko, A.I. Poddel'sky, A.S. Bogomyakov, N.V. Somov, G.A. Abakumov, V.K. Cherkasov, *Polyhedron* 49 (2013) 239.
- [34] P. Rabu, J.-M. Rueff, Z.-L. Huang, S. Angelov, J. Souletie, M. Drillon, *Polyhedron* 20 (2001) 1677.
- [35] (a) J.M. Rueff, N. Masciocchi, P. Rabu, A. Sironi, A. Skoulios, *Eur. J. Inorg. Chem.* (2001) 2843;
(b) J.M. Rueff, N. Masciocchi, P. Rabu, A. Sironi, A. Skoulios, *Chem. Eur. J.* 8 (2002) 1813.
- [36] T.L. Hu, J.J. Wang, J.R. Li, X.H. Bu, *J. Mol. Struct.* 796 (2006) 18.
- [37] J. Zhang, Y.R. Xie, Q. Ye, R.G. Xiong, Z. Xue, X.Z. You, *Eur. J. Inorg. Chem.* (2003) 2572.
- [38] (a) Y. Cui, Y. Yue, G. Qian, B. Chen, *Chem. Rev.* 112 (2012) 1126;
(b) J. Lu, K. Zhao, Q.R. Fang, J.Q. Xu, J.H. Yu, X. Zhang, H.Y. Bie, T.G. Wang, *Cryst. Growth Des.* 5 (2005) 1091.
- [39] (a) N. Sun, Y. Yan, J. Chen, *J. Mol. Struct.* 1047 (2013) 324;
(b) P.-P. Yang, B. Li, Y.-H. Wang, W. Gu, X. Liu, Z. Anorg. Allg. Chem. 634 (2008) 1221.